DESIGN OPTIMIZATION OF CENTRAL AND DECENTRAL UNITS IN DECARBONIZED DISTRICT HEATING NETWORKS

Maximilian Sporleder[1,2]*, Michael Rath[1,3], Mario Ragwitz[1,2]

[1] Fraunhofer IEG, Fraunhofer Research Institution for Energy Infrastructures and Geothermal Systems, Cottbus, Germany

[2] Brandenburg University of Technology Cottbus-Senftenberg (BTU CS), Cottbus, Germany

[3] Bochum University of Applied Sciences, Bochum, Germany

*Corresponding Author: maximilian.sporleder@ieg.fraunhofer.de

ABSTRACT

Climate change forces district heating operators to reduce their CO_2-emissions and decarbonize their district heating systems (DHSs). A solution for a decarbonized system might be the combination of central and decentral units. This combination offers the possibility to supply each consumer with their individual temperature.
However, it raises the question of the optimal design between central and decentral units and how they perform against a central supply. Therefore, a mixed-integer linear programming (MILP) model was developed capable of designing and operating several supply systems inside the network at different locations – decentralized and centralized. In this study, the combined system is compared to a central supply. Every energy converter's and storage's design and operation are optimized based on an objective function, minimizing the total system cost consisting of the annuity of operational and capital expenditures (opex and capex). The model can select central options such as a buffer tank, photovoltaic (PV) field, combined heat and power (CHP) plant, biomass boiler, large-scale wastewater heat pump (WWHP), and a solar thermal field. The combined system additionally designs booster heat pumps – other decentral options are not viewed in this study. The optimization horizon is one year in 24 h timesteps. The MILP method and all necessary component models are implemented as an open-source Python package.
The method was applied in a case study with a district heating network (DHN) supplying 22 buildings distributed into six classes. Every class has a demand and supply temperature curve. In this study, different temperature levels and electricity prices were investigated. The results show that the combined system of central and decentral units performs best at a maximum network temperature of 85 °C, installing booster heat pumps only at high-temperature buildings. The combined system can distribute the temperature's lift, increasing the coefficient of performance (COP) for the central heat pump. Furthermore, the lowered network temperature decreases the investment for the WWHP because a second compressor stage is no longer needed. The best configurations supply heat between 14 ct/kWh and 16 ct/kWh.

1 INTRODUCTION

Global climate change is one of the biggest threats in the 21st century. It is not only a threat due to more extreme weather conditions but also due to the costs caused by these events. Newman and Noy (2023) found that US$ 143 billion per year is attributed to extreme weather events caused by climate change. Renewable DHNs are a promising approach to reduce greenhouse gas emissions and decarbonize the energy system.
DHNs offer a cost-effective and flexible solution for large-scale utilization of low-carbon energy for heating purposes (International Energy Agency, 2023). However, the decarbonization potential of district heating is largely untapped, as 90 % of the heat supplied in district networks is produced from

https://doi.org/10.52202/077185-0064

fossil fuels, especially in the two largest markets of China and Russia (International Energy Agency, 2023). Aligning with the Net Zero Emissions by 2050 (NZE) Scenario requires significantly stronger efforts to rapidly improve the energy efficiency of existing networks and switch them to renewable heat sources (such as bioenergy, solar thermal, large-scale heat pumps, and geothermal) (International Energy Agency, 2023).
Especially supplying heterogeneous demand strutures is challenging for district heating operators because the consumers get the same temperature from the network. A solution might be to combine central units with booster heat pumps, satisfying the individual needs of consumers connected to the network. In order to support the operators, a tool was developed to answer the research question: How can a planer optimize the design of a DHS, including central units and booster heat pumps connected by a network?

1.1 State-of-the-Art

The heat supply via DHNs has evolved over the decades, developing from a central supply system to a combination of central and decentral units. Lund *et al.* (2021) include several renewable heat supply technologies in the 4th generation of DHNs, such as PV, solar thermal fields, biomass, CHP powered by biogas, centralized heat pumps, and others. The transition from the 3rd to the 4th generation requires lowering the network's supply temperature in order to integrate renewable heat sources efficiently (Lund *et al.*, 2021). The needed supply temperature of the building dictates the network's temperatures. Hummel *et al.* (2021) identified a high potential for refurbishing the building structure in several European countries. Suppose the refurbishment leads to a heterogeneous demand structure due to different temperature needs. In that case, operating the network at lower temperatures and lifting the temperature inside the building can be a more efficient approach. Lund *et al.* (2021) described this concept as 5th generation. Wirtz *et al.* (2020) not only included the combination of central and decentral units in their optimization but also parallel heating and cooling. However, this research focuses on the network and its temperature with a heterogeneous demand structure.
Rämä and Wahlroos (2018) investigated the effects of a new decentralized renewable heat supply in an existing DHS. They performed a case study for Helsinki evaluating the techno-economic performance of decentralized heat pumps and solar collectors for different temperature levels. Utilizing EnergyPro as a modeling tool, they found that CHP-based heat production is set to decrease 68-73 % by 2030. In this study, different temperature levels are also examined for a combined supply system of central and decentral units. In addition, this study adds a spatial discretization for the exact position of the decentral unit's installation and implements an optimized design for the energy converters and storages.
Huang *et al.* (2017) developed a model to coordinate the dispatch of electric power and DHNs utilizing decentral units. The model is an optimality condition decomposition and connects the electric grid with two DHNs via two CHP plants. The DHN was connected to a thermal storage for dispatch. In this work, CHP plants are also included as part of the central system; however, this study focuses more on the design optimization for the supply system than the operation, as Huang *et al.* (2017) did.
Nuytten *et al.* (2013) investigated the flexibility of CHP plant systems. The focus was the effect of centralized vs. decentralized storages on thermal systems. They found that an increasing CHP plant does not increase the system's flexibility, while the buffer tank size has an almost linear influence on the flexibility (Nuytten *et al.*, 2013). This study optimizes the design of the supply system, making it unnecessary to test different buffer tank sizes.
Gratiela *et al.* (2022) examined a similar research question connecting a central supply system with a DHN and using decentral booster heat pumps to lift the temperature inside the building. They simulated scenarios investigating different energy mixes with a fixed temperature development for the DHN. This study contributes to their work by developing an optimization and analyzing different temperature levels in the demand structure.
Morvaj *et al.* (2016) developed a MILP model optimizing the system's design, operation, and layout of the DHN. They minimized CO_2-emissions and costs in a multi-objective optimization. The energy hub supplying heat consisted of a PV field, CHP plant, gas boiler, solar thermal field, and a buffer tank. The central supply in this study has a similar system with an additional WWHP. However, the

https://doi.org/10.52202/077185-0064

model introduced in the method section can also deselect a component. In addition to Morvaj *et al.*'s (2016) work, this study also designs decentral units and considers the network's temperature.
Mertz *et al.* (2016) developed a mixed-integer nonlinear problem optimizing the network design. The goal was to minimize the operating costs of the network and its investments. They depicted the network into nodes and edges, similar to Krug *et al.* (2020). In contrast to Krug *et al.* (2020), they used an exponential description to calculate the temperature losses inside the pipe. In this study, the formulation provided by Krug *et al.* (2020) to describe the thermal energy balance for each pipe was used.
Mu *et al.* (2020) focused on the optimal dispatch for an integrated energy system with multiple plants. They optimized the operation and utilized waste heat, improving the system's energy efficiency.
Sporleder *et al.* (2023) added design optimization to the operation optimization for all energy converters and storages. The MILP model was limited to central units. This study wants to complement Sporleder *et al.*'s (2023) work by integrating decentral units into the MILP model. Based on the state-of-the-art this research paper wants to contribute with

- a generic and open-source MILP model capable of optimizing the dimension and operation of central and decentral units in a DHN,
- different temperature levels and electricity prices and their effect on the design of a DHN with a central supply (referred to as the central system) and a DHN supported by booster heat pumps (referred to as the combined system) are investigated for a heterogeneous demand structure.

The paper follows up with the method section, explaining the mathematical formulation for designing the decentral units, extending the approach by Sporleder *et al.* (2023). In the result section, the method is applied to a case study examining different electricity prices. This study continues by discussing the results and concludes with the most important findings.

2 METHOD

This section explains the most important equations used in the MILP model and the altered equations from the existing literature. Figure 1 shows the DHN for this research with the different building classes. The DHN is an existing network in Germany. Due to confidential reasons, the topology was slightly changed. Each building class has a minimum and maximum supply temperature depending linearly on the ambient temperature (see **Table 1**). Due to the time step of 24 h, the maximum supply temperature can be lower than, e.g., 95 °C for the big house building class because averaging the time series data leads to lower maximum and minimum values.

Table 1: Needed supply temperature, demand, and frequency of occurrence for each building class

Building class	Frequency	Minimum temperature at warmest ambient temperature	Maximum temperature at coldest ambient temperature	Maximum demand
Kindergarten	1	60 °C	70 °C	42 kW
Small house	12	60 °C	75 °C	55 kW
School	1	60 °C	80 °C	95 kW
Middle house	5	65 °C	85 °C	110 kW
Hospital	1	70 °C	90 °C	256 kW
Big house	2	75 °C	95 °C	220 kW

The method is a MILP model minimizing the annuity of capex and opex. The MILP model from Sporleder *et al.* (2023) was extended, depicting booster heat pumps at the consumers. The Python package can be found under Fraunhofer IEG (2023) in the branch *decentral*. The time horizon is one year – 2030 – within 24 h time steps. The economic calculation is based on the annuity method (VDI The Association of German Engineers, 2012). In the following, the most important equations are

https://doi.org/10.52202/077185-0064

introduced and the changes made to the model. A very detailed description of the model can be found in Sporleder *et al.* (2024).

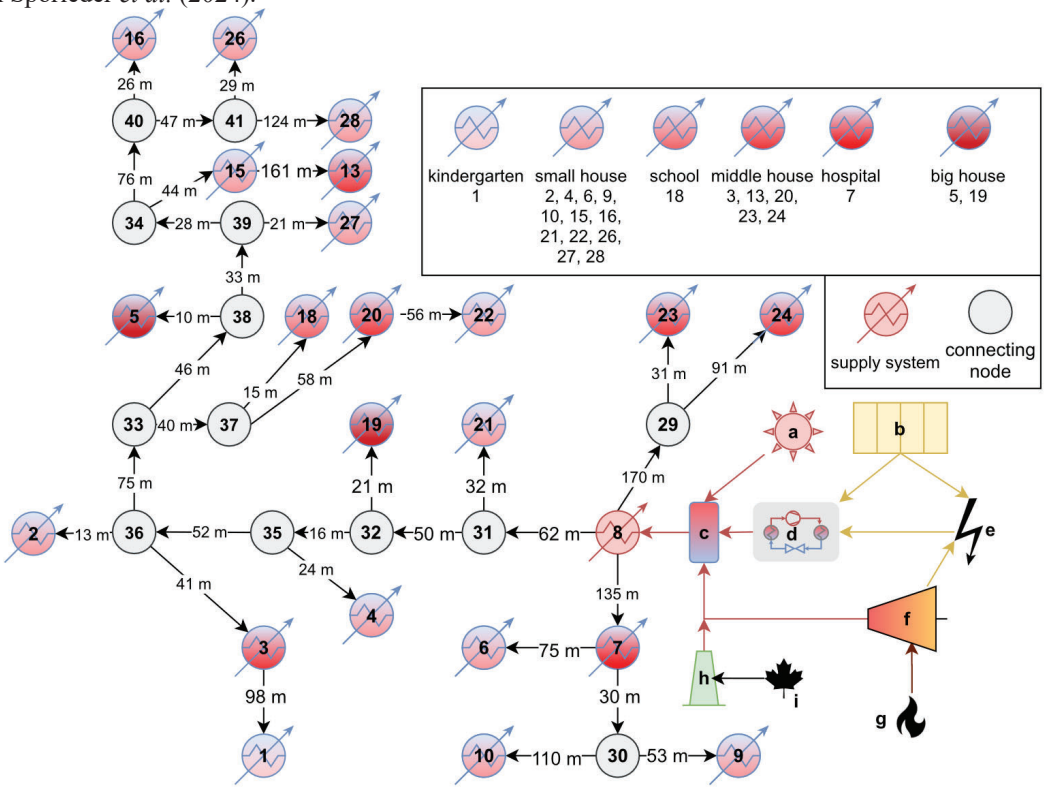

Figure 1: Depiction of the case study's DHN with the six building classes in the top, with rising temperature level from left to right; at position eight is the central integration point with a) solar thermal field, b) PV field, c) buffer tank, d) WWHP, e) electric grid, f) CHP plant, g) biogas, h) biomass boiler, i) biomass

The method is divided into two problems: a hydraulic optimization for the network to calculate the resulting mass flows and a design optimization problem. Separating the problem allows a linear description of the design optimization for the network because the mass flows become parameters. In the design optimization, the temperature inside the DHN is a variable. After the first run of the design optimization, the thermal efficiencies are recalculated, e.g., COPs for heat pumps. Then, the design optimization runs a second time, where the temperature is again a variable. The objective function of the design optimization problem is given by Equation (1) (Sporleder *et al.*, 2023)

$$\min\left(f^{\text{opex,var}}, g^{\text{opex,fix}}, h^{\text{capex}}\right), \tag{1}$$

where the variables investment costs h^{capex}, variable opex $f^{\text{opex,var}}$, and fixed opex $g^{\text{opex,fix}}$ are minimized. The opex include the sum of all operational costs over the given time horizon. The dimension of each device influences its investment. Depending on the nominal dimension of the decentral unit $\dot{Q}_a^{\text{decentral,nom}}$, the capex h^{capex} in the objective function increase. The capex also includes the equipment of the central supply. Each device has a buying decision represented as an auxiliary variable. The central heat pump has a control auxiliary variable for each timestep. All other variables are continuous. The equipment's specific capex and other techno-economic information were extracted from the Danish Energy Agency (2024). The electricity price is from 2023 in Germany – on average 9.5 ct/kWh. Additional allocations are added separately – ca. 4 ct/kWh for the central heat pump and 7 ct/kWh for the booster heat pumps. The electricity price is given as a time series. Each pipe has an energy balance represented by Equation (2) (Sporleder *et al.*, 2023)

https://doi.org/10.52202/077185-0064

$$c_{\mathrm{p}} m_a \frac{T_{a,t-1}^{\mathrm{out}} - T_{a,t}^{\mathrm{out}}}{\Delta t} + \dot{m}_{a,t} c_{\mathrm{p}} \left(T_{a,t}^{\mathrm{in}} - T_{a,t}^{\mathrm{out}}\right) - U_a A_a^{\mathrm{m}} \left(T_{a,t}^{\mathrm{out}} - T_t^{\mathrm{soil}}\right) = 0 \;\; for\; a \in Z^{\mathrm{ff}}, Z^{\mathrm{bf}}, t \in \tau, \tag{2}$$

where the mass m_a, the outlet temperature $T_{a,t}^{\mathrm{out}}$, the timestep Δt, and the specific heat capacity c_{p} can express the pipe's energy storage. The mass flow $\dot{m}_{a,t}$ comes from the hydraulic optimization; therefore, Equation (2) is a linear constraint. The inlet temperature is denoted as $T_{a,t}^{\mathrm{in}}$. The soil temperature T_t^{soil}, the heat transfer coefficient U_a, the pipe's surface A_a^{m}, and the outlet temperature determine the pipe's heat loss.

The thermal output from the central supply is given by Equation (3) (Sporleder *et al.*, 2023)

$$\mu_a^{\mathrm{pro}} \left[\dot{m}_{a,t} c_{\mathrm{p}} \left(T_{a,t}^{\mathrm{out}} - T_{a,t}^{\mathrm{in}}\right)\right] = \sum_{k \in Z^{\mathrm{conv}}(a)} \dot{Q}_{k,t}^{\mathrm{conv}} + \sum_{k \in Z^{\mathrm{stor}}(a)} \left(\dot{Q}_{k,t}^{\mathrm{out,stor}} - \dot{Q}_{k,t}^{\mathrm{in,stor}}\right) \quad for\; t \in \tau, a \in Z^{\mathrm{pro}}, \tag{3}$$

where the mass flow $\dot{m}_{a,t}$ enters the heat exchanger with the inlet temperature $T_{a,t}^{\mathrm{in}}$ and leaves it with the outlet temperature $T_{a,t}^{\mathrm{out}}$. The heat exchanger's efficiency is denoted as μ_a^{pro}. The sum of the energy converter's heat flow $\dot{Q}_{k,t}^{\mathrm{conv}}$ is added to the subtraction of storage discharging $\dot{Q}_{k,t}^{\mathrm{out,stor}}$ and charging $\dot{Q}_{k,t}^{\mathrm{in,stor}}$.

The operation of the decentral units influences the variable opex $f^{\mathrm{opex,var}}$ in the objective. In Sporleder *et al.* (2023), the energy balance of the consumer was given by Equation (4)

$$\frac{\dot{Q}_{a,t}^{\mathrm{con}}}{\mu^{\mathrm{con}}} = \dot{m}_{a,t} c_{\mathrm{p}} \left(T_{a,t}^{\mathrm{in}} - T_{a,t}^{\mathrm{out}}\right) \quad for\; t \in \tau, a \in Z^{\mathrm{con}}, \tag{4}$$

where $\dot{Q}_{a,t}^{\mathrm{con}}$ is the heat demand, $\dot{m}_{a,t}$ is the mass flow in the network at the consumer, $T_{a,t}^{\mathrm{out}}$ is the temperature leaving the consumer and $T_{a,t}^{\mathrm{in}}$ is the entering temperature. The entering temperature was defined as $T_{a \in Z^{\mathrm{con}},t}^{\mathrm{in}} \geq T_{a \in Z^{\mathrm{con}},t}^{\mathrm{supply}}$, where $T_{a \in Z^{\mathrm{con}},t}^{\mathrm{supply}}$ is the supply temperature needed inside the building. For the model with decentral units, Equation (4) changes to Equation (5)

$$\frac{\dot{Q}_{a,t}^{\mathrm{con}}}{\mu^{\mathrm{transfer}}} \leq P_{a,t}^{\mathrm{decentral,el}} + \dot{m}_{a,t} c_{\mathrm{p}} \left(T_{a,t}^{\mathrm{in}} - T_{a,t}^{\mathrm{out}}\right) \quad for\; t \in \tau, a \in Z^{\mathrm{con}}, \tag{5}$$

where $P_{a,t}^{\mathrm{decentral,el}}$ is the electric input into the heat pump. The right term is the network's thermal power, and it reacts as a heat source for the heat pump. The thermal power of the network plus the electric power of the decentral heat pump lead to the thermal power output of the heat pump $\dot{Q}_{a,t}^{\mathrm{decentral}}$. This has to be bigger than the building's demand. μ^{transfer} is the efficiency of the heat transfer at the house station.

The allowed temperature inside the network is reduced by 5 K, from 95 °C to 65 °C, forcing the optimizer to build decentral booster heat pumps. Additionally, a minimum temperature at this consumer is ensured with Equation (6)

$$P_{a,t}^{\mathrm{decentral,el}} + \dot{m}_{a,t} c_{\mathrm{p}} \left(T_{a,t}^{\mathrm{in}} - T_{a,t}^{\mathrm{out}}\right) \geq \dot{m}_{a,t} c_{\mathrm{p}} \left(T_{a,t}^{\mathrm{supply}} - T_{a,t}^{\mathrm{out}}\right) \quad for\; t \in \tau, a \in Z^{\mathrm{con}}. \tag{6}$$

The decentral unit is further limited by Equation (7)

$$\dot{Q}_{a,t}^{\mathrm{decentral}} \leq \dot{Q}_{a,t}^{\mathrm{con}} \quad for\; t \in \tau, a \in Z^{\mathrm{con}}. \tag{7}$$

The dimension of a decentral unit $\dot{Q}_a^{\mathrm{decentral,nom}}$ is defined by Equation (8)

$$\dot{Q}_{a,t}^{\mathrm{decentral}} \leq \dot{Q}_a^{\mathrm{decentral,nom}} \quad for\; t \in \tau, a \in Z^{\mathrm{con}}. \tag{8}$$

The opex for the booster heat pump depends on the thermal power and the COP. The MILP model runs twice, and in the first run, the source temperature – here $T_{a,t}^{\mathrm{out}}$ – is estimated, and in the second run, the source temperature is taken from the first run's results. Then, the COP is calculated as a time series a priori based on the Carnot efficiency with a fixed quality grade of 0.4 for WWHPs and 0.5 for water-to-water heat pumps. The opex is then calculated with Equation (9-10)

$$C_a^{\mathrm{opex,var}} = \Delta t \sum_{t \in \tau} \left(\dot{Q}_{a,t}^{\mathrm{decentral}} c^{\mathrm{opex,var}} + \frac{\dot{Q}_{a,t}^{\mathrm{decentral}}}{COP_{a,t}} c_t^{\mathrm{electric}}\right) for\;\; a \in Z^{\mathrm{decentral}}, \tag{9}$$

$$C_a^{\mathrm{opex,fix}} = \dot{Q}_a^{\mathrm{decentral,nom}} c^{\mathrm{opex,fix}} \;\; for\;\; a \in Z^{\mathrm{decentral}}, \tag{10}$$

https://doi.org/10.52202/077185-0064

where $c^{\text{opex,var}}$ is the specific variable opex, $c^{\text{opex,fix}}$ is the fixed opex and $C_a^{\text{opex,var/fix}}$ is the opex over the time horizon for one booster heat pump. The fixed opex $C_a^{\text{opex,fix}}$ is added to the overall fixed opex $g^{\text{opex,fix}}$. The same is done for the variable opex $C_a^{\text{opex,var}}$. The constraints are unchanged for the other energy system components (Sporleder *et al.*, 2023). The data for the model can be taken from Fraunhofer IEG (2023). The electricity price c_t^{electric} is a fluctuating curve with an average price of 9.5 ct/kWh. The biomass and biogas price is 14 ct/kWh (Pfluger *et al.*, 2023).
In addition, equations were implemented to increase the capex for a heat pump if a second compressor stage is needed. Every central heat pump has an auxiliary control variable $u_{i,t}$. If the heat pump is operated while lifting the fluid's temperature greater than 75 K, a decision variable γ_i for the second stage is set to 1, defined by Equation (11)

$$\sum_{t \in \tau^{\text{critical}}} u_{i,t} \leq \gamma_i n(\tau) \quad for\ i \in Z^{\text{heat pump}} \tag{11}$$

where τ^{critical} is the number of time steps where the temperature delta between sink and source is greater than 75 K and $n(\tau)$ is the number of time steps. If γ_i is 1, the capex for the heat pump increases by 60 %.
The pipes' capex C_i^{pipe} are defined by (Pfluger *et al.*, 2023)

$$C_a^{\text{pipe}} = 158.11 {D_a^{\text{pipe}}}^{0.3969} L_a^{\text{pipe}} \quad for\ a \in Z^{\text{pipe}}, \tag{12}$$

where D_a^{pipe} is the diameter of each pipe given in mm, and L_a^{pipe} is the length of each pipe in m. It is assumed that the network is newly installed and the capex are added to h^{capex}.

3 RESULTS

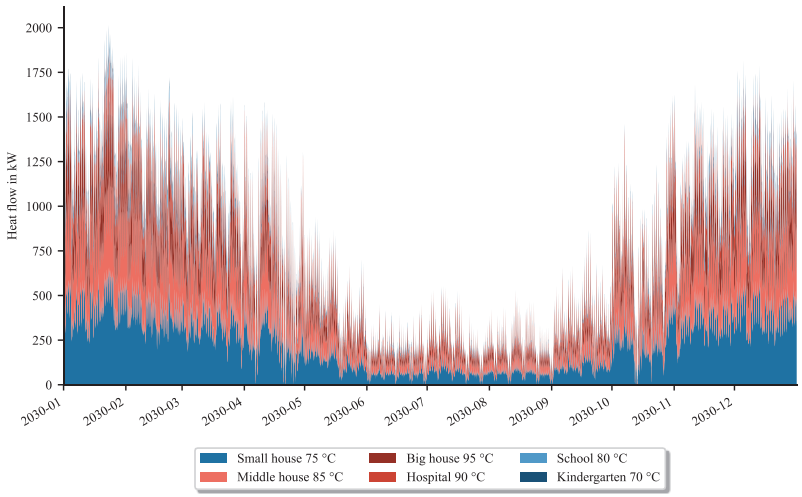

Figure 2: Summed up demands for the different building classes with their respective max. supply temperature

The result section compares the central system with a combined system. The case study can be seen in **Figure 1**. The optimizer can choose from a WWHP, a solar thermal and PV field (each max. 300 m^2), a CHP plant fired with biogas, a biomass boiler, and a buffer tank (max. 100 m^3). The PV field and the CHP plant can deliver electricity to the WWHP or sell it to the grid. The WWHP has a constant heat source with 15 °C and pays 1 ct/kWh_{th} for this heat source. The network is newly installed, and the investment is in the total system cost. The demand structures consist of one kindergarten, one school, one hospital, and 19 housings divided into three building classes. The smallest building occurs 12 times, the middle building five times, and the big building twice. **Figure 2** shows the stacked demands over all buildings differentiated into their classes. The building class small house has a relatively low supply temperature, and this building class occurs more often than other classes,

https://doi.org/10.52202/077185-0064

leading to the highest summed-up demand. The building class big house has a relatively high temperature but only occurs twice, leading to a smaller summed-up demand. The maximum temperature required in the summer is 75 °C. The network's temperature is limited in 5 K steps, starting at 95 °C and reducing to 65 °C.

3.1 Techno-Economic Analysis for the Base Scenario

For the analysis, the DHS in **Figure 1** is optimized once with only central units as a supply system and then with a maximum temperature of 75 °C inside the network. The electricity price from 2023 (on average 9.5 ct/kWh) is gradually decreased by 1 ct/kWh and, at maximum by 4 ct/kWh.
In the base scenario with a central supply system without any electricity price change, the optimizer dimensions a WWHP with 1.78 MW, a CHP plant with 0.39 MW_{th}, a solar thermal field with 300 m^2, a PV field with 300 m^2, and a buffer tank with 100 m^3. The energy mix is shown in **Figure 3**a). The WWHP covers the majority due to the favorable heat source and the space limitation for the solar thermal field. The buffer tank balances out the fluctuations in the electricity price. The total system cost, including all the equipment – network, transfer/house stations, etc. – is 14.65 ct/kWh.

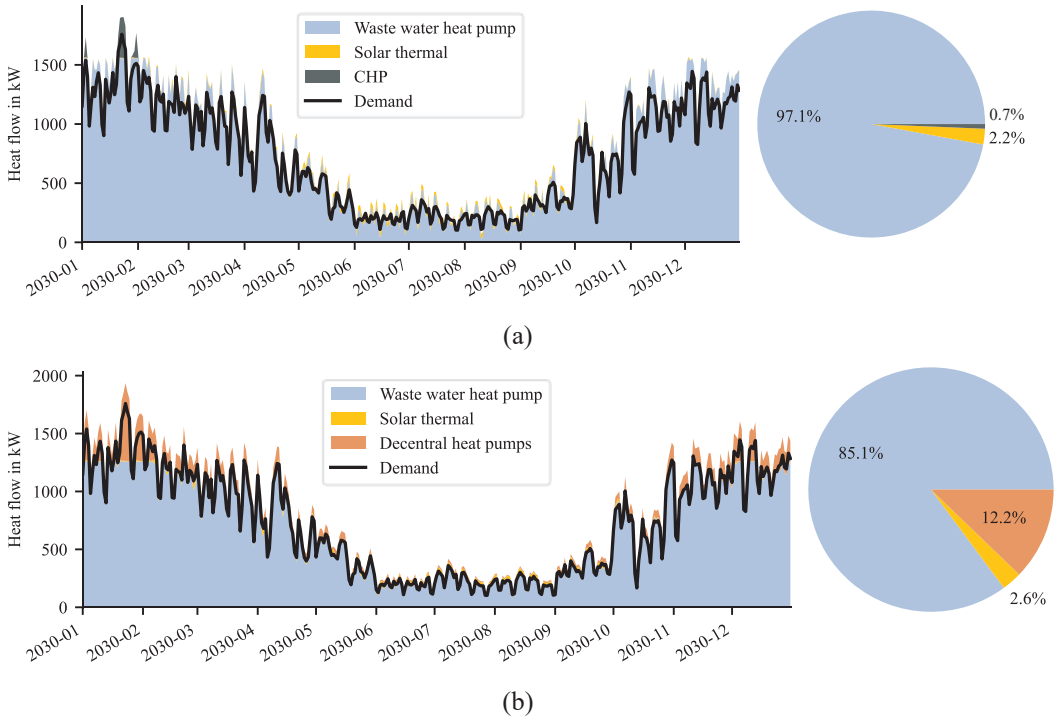

Figure 3: Energy mix for the a) central supply and the b) combined supply for no electricity price change

For the option of decentral units, the energy mix changes and shifts a small load inside the buildings (12.2 %). The optimizer designs a WWHP with 1.44 MW, and a PV and solar thermal field with respectively 300 m^2. The solar thermal field has a higher energy output with 187.6 MWh compared to the solar thermal field installed in the central system with 161 MWh. A lower network temperature and an increased thermal efficiency for the solar thermal field cause this higher energy output. The mean injection temperature at node 8 is 75 °C in the combined system, while the mean injection temperature in the central system is 87 °C. The lower temperature in the combined system causes 17 % less thermal losses.
Furthermore, the seasonal COP of the WWHP increases from 2.46 to 3, and the specific capex declines from 1,529 €/kW to 1,156 €/kW because the temperature delta between sink and source decreases, and no second compressor stage is needed.

https://doi.org/10.52202/077185-0064

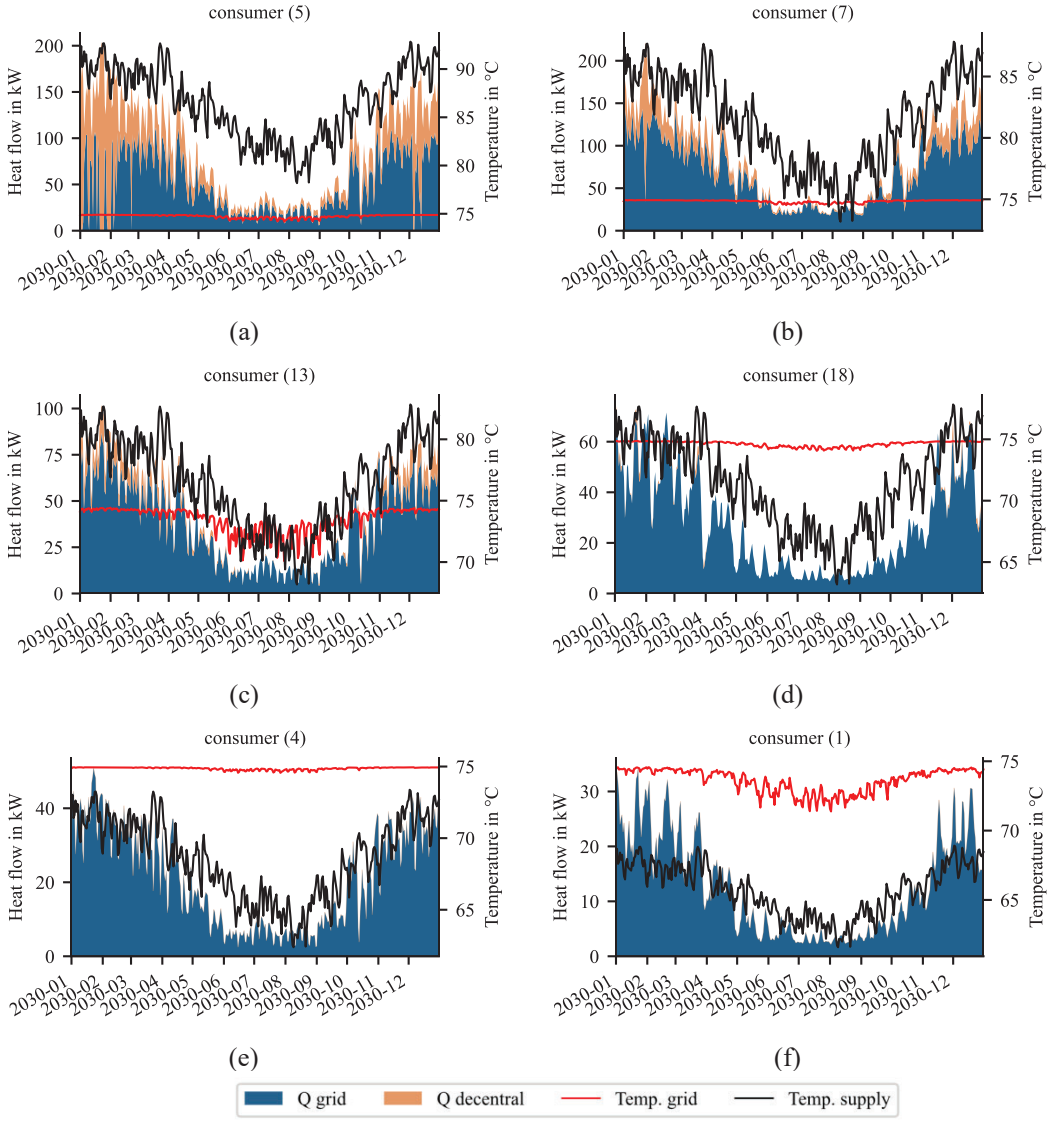

Figure 4: The energy supply for different building classes showing the share of thermal power from the network/grid and the decentral units on the left y-axis; showing the network/grid's temperature and the needed supply temperature on the right y-axis for building class a) big house, b) hospital, c) middle house, d) school, e) small house, f) kindergarten

At the building class kindergarten and small house, no decentral unit is installed except for building number 28 because it is at the network's end. The installation of the decentral units increases the total capex by 29 %. This leads to a total system cost of 17.34 ct/kWh. The booster heat pumps are smaller and specifically more expensive than the central supply heat pump.

Figure 4 shows six consumer locations, each depicting a building class. The plot differentiates between the thermal power coming from the network and the power added by the decentral heat pumps. On the right y-axis, the temperature at the transfer station is shown together with the needed supply temperature. The temperature at the consumers is relatively constant at 75 °C.

Figure 4a) shows the consumer at location 5 from the big house building class. The supply temperature mostly fluctuates between 75 °C and 95 °C, resulting in a seasonal COP of 2.5. The mass

https://doi.org/10.52202/077185-0064

flow is at 0.45 kg/s. The share of supplied energy by the grid is 60 %, and the share of supplied energy by the booster heat pump is 40 %.
Figure 4b) shows the consumer at location 7 from the hospital building class. The supply temperature mostly fluctuates between 70 °C and 90 °C, resulting in a seasonal COP of 5.1. The network's temperature at this location is between 70 °C and 79 °C. The share of supplied energy by the network is 80.5 %, and the share of supplied energy by the decentral units is 19.5 %. The mass flow is similar to consumer 5.
Figure 4c) illustrates the thermal power at consumer 13 from the building class middle house. The seasonal COP increases to 9 compared to consumer 7. The share of supplied energy by the grid increases to 89.1 %. The consumer receives a mass flow rate of 0.27 kg/s due to the more considerable distance to the central supply station and the reduced number of consumers on that line.
Figure 4d) shows consumer 18 with a network share of 98.5 %, and it is questionable to install a decentral unit for the missing temperature lift.
Figure 4e) and f) depict consumers 4 and 1 from the small house and the kindergarten building class. At these locations, the thermal power and temperature supplied by the network are sufficient; therefore, no decentral unit is installed.

3.2 Techno-Economic Analysis for Different Electricity Prices

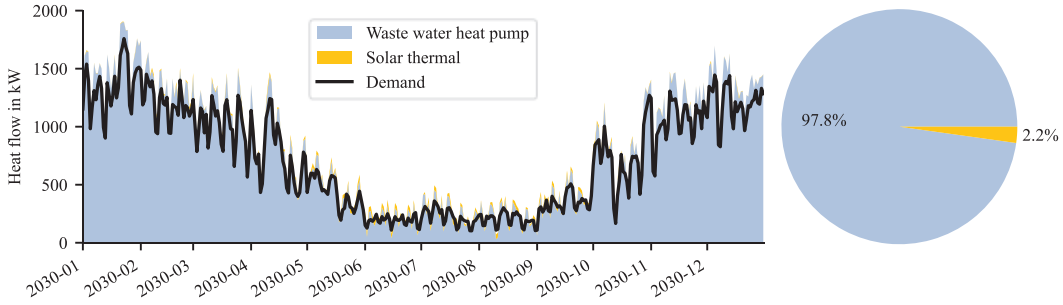

(a)

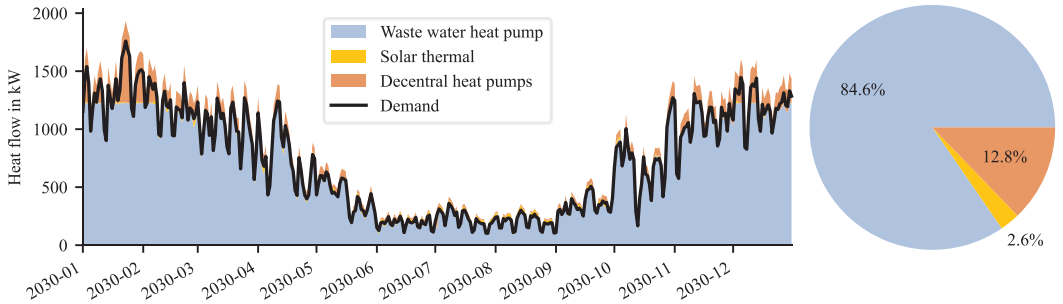

(b)

Figure 5: Energy mix for the a) central supply and the b) combined supply for a maximum network temperature of 75 °C and an average electricity price of 5.5 ct/kWh

Figure 5 shows the energy mix for a) the central supply and b) the combined supply of central and decentral units for an average electricity market price of 5.5 ct/kWh. It should be noted that the allocations are added to this price. The network's temperature is limited to 75 °C in the combined system.
The central system no longer installs a CHP plant (390 kW_{th} in the base scenario) due to the lowered electricity price. In the base scenario, the CHP plant is used to supply electricity during peak prices. For a lower electricity price, the WWHP buys the electricity from the energy market instead of relying on the CHP plant. The solar thermal and PV field have a dimension of 300 m^2. The total system cost decreases to 12.9 ct/kWh. The network's mean injection temperature at node 8 stays at 87 °C.

https://doi.org/10.52202/077185-0064

In the combined system, the injection temperature stays at 75 °C. The decentral supply is increased slightly by 0.6 %. The WWHP is decreased to 1.4 MW compared to 3.1. The total system cost decreases by 2 ct/kWh to 15.33 ct/kW compared to the combined system in the base scenario – section 3.1.
Figure 6 shows the development of the total system cost dependent on the network temperature. Furthermore, four electricity price reductions are plotted. Lowering the electricity price, leads to lower total system cost for generating and distributing the heat. The system is dominated by Power-to-Heat technologies, which depend on the electric market. For the 65°C scenario, the 9.5 ct/kWh$_{el}$ scenario is close to the 8.5 ct/kWh$_{el}$ scenario. This can happen due to the optimization gap (2 %) and the close values.

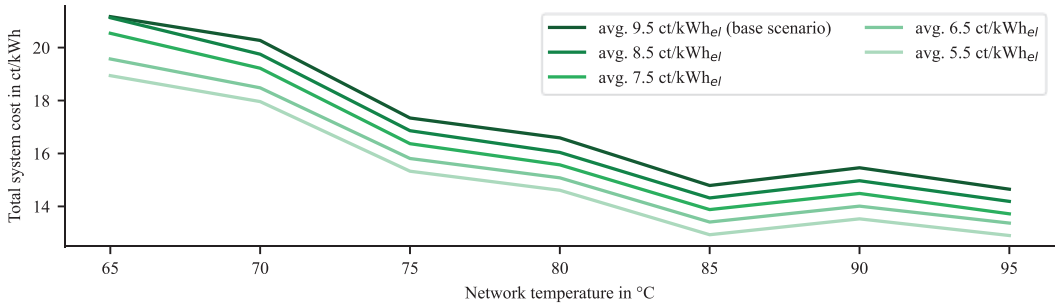

Figure 6: Development of the total system cost depending on the network temperature for an average electricity price of 9.5 ct/kWh$_{el}$, 8.5 ct/kWh$_{el}$, 7.5 ct/kWh$_{el}$, 6.5 ct/kWh$_{el}$, and 5.5 ct/kWh$_{el}$

For the 85 °C scenario, the total system cost for the heat supply decreases. In this scenario, a booster heat pump supports buildings 5, 7, and 19. These buildings belong to the buildings classes big house and hospital requiring relatively high temperatures – see **Figure 4**a) and b). The WWHP only needs one compressor stage in this scenario, leading to a specific capex of 1137 €/kW. The seasonal COP is at 2.6. For an electricity price of 6.5 ct/kWh$_{el}$, the total system is 13.4 ct/kWh. With the installation of decentral booster heat pumps, the buffer tank is never installed.

4 DISCUSSION

The combined system performs best when installing booster heat pumps for the buildings with the highest demand temperatures (see building classes big house and hospital). The leading cause is the demand structure given in the case study. Only three buildings demand a temperature above 85 °C, while 35 % of the buildings can be sufficiently supplied with temperatures between 60 °C and 75 °C. However, further lowering the network's temperature leads to installing booster heat pumps in almost every building, significantly increasing investments. One key factor is the compressor stage of the central heat pump. The investments decline if the heat pump can lift the heat source's temperature to the network temperature in one stage. Therefore, it should be essential to reduce the temperature of future DHN to a level where heat pumps utilizing environmental heat do not require a second compressor stage. Additionally, the COP increases, leading to reduced opex.
The results have also shown that installing booster heat pumps at a few locations can be economical for a heterogeneous demand structure. Another solution could be refurbishing the buildings and lowering the building's demanding temperature. In the future, buildings requiring significantly higher temperatures, which need booster heat pumps, could receive an individual price tag. This temperature-dependent price inside a DHN could incentivize owners to refurbish their buildings. A refurbishment option could be integrated into the optimization, further advancing the tool and the options for a planner.

https://doi.org/10.52202/077185-0064

5 LIMITATION OF RESULTS

In the optimization, the thermal calculation is performed after the hydraulic calculation in order to linearize the model. Performing the optimization with temperatures and mass flows inside the network will always lead to nonlinearities. Therefore, the two problems were separated, which has often been done in the literature (Sporleder *et al.*, 2022).
Furthermore, the chosen time step is set to 24 h, which is relatively long. However, this research focuses on designing, and the time step and the time horizon should be chosen smaller for an operation optimization. On top of that, the calculation of all scenarios took 24 h, resulting in a need for a reduced problem size. The same model was applied by Sporleder *et al.* (2024), and they evaluated the effect on the design of the supply system extensively. They concluded that it majorly affects energy converters that supply peak loads and, therefore, introduced a scaling factor to increase the dimension of these energy converters. The calculation and explanation can be found in Sporleder *et al.* (2024). The same factor (0.145) was applied in this research. Nevertheless, the increase in the timely resolution is an essential point for future research.
The decentral booster heat pump is calculated with a simplified energy balance, neglecting the resulting temperature leaving the condenser. This temperature might be higher than the needed supply temperature inside the building, causing the need for additional storage units. However, this simplification does not change the qualitative outcome of the results. Installing booster heat pumps in a few buildings with a high demanding temperature increases the system's efficiency and lowers costs.
Furthermore, the temperature reduction step is set to 5 K. A smaller reduction could lead to slightly different results. Unfortunately, a smaller step of the temperature reduction would also lead to much higher computational time because more scenarios would be generated; therefore, 5 K was chosen as a temperature reduction. The results still indicate a trend that can be seen for the 85 °C scenario.

6 CONCLUSION AND FUTURE RESEARCH

In this research, a MILP model was developed to design central and decentral units inside a DHN. The decentral units lift the fluid's temperature to the needed supply temperature. This concept of a combined system was compared to a central system and applied to a case study.
The main findings are that the combined system performs economically best under the given demand structure at a maximum network temperature of 85 °C. Network operators should aim for temperatures low enough to integrate heat pumps with one compressor stage. If only a few buildings require a high temperature, installing booster heat pumps at these locations can increase the system's economics. Installing booster heat pumps in all buildings and further lowering the network's temperature results in a total system cost for heating above 20 ct/kWh. The best configurations in this study reach total system cost for heating between 14 ct/kWh and 16 ct/kWh.
In the future, refurbishment could be viewed inside the optimization to increase the options and the system's energy efficiency. Additionally, the computational time should be decreased and the timely resolution increased in future research.

REFERENCES

Danish Energy Agency (2024), Technology Data for Energy storage, available at: https://ens.dk/en/our-services/technology-catalogues (accessed 7 March 2024).

Fraunhofer IEG (2023), Heatopia, available at: https://gitlab.cc-asp.fraunhofer.de/max02865/heatopia.git (accessed 16 November 2023).

Gratiela, T., Mioara, V. and Florin, T. (2022), Ecological Refrigerant Cascade Systems Replacement in Accordance with the EU Regulations, CLIMA 2022 conference, 2022: CLIMA 2022 The 14th REHVA HVAC World Congress.

Huang, J., Li, Z. and Wu, Q.H. (2017), Coordinated dispatch of electric power and district heating networks: A decentralized solution using optimality condition decomposition, *Applied Energy*, Vol. 206, pp. 1508–1522.

https://doi.org/10.52202/077185-0064

Hummel, M., Büchele, R., Müller, A., Aichinger, E., Steinbach, J., Kranzl, L., Toleikyte, A. and Forthuber, S. (2021), The costs and potentials for heat savings in buildings: Refurbishment costs and heat saving cost curves for 6 countries in Europe, *Energy and Buildings*, Vol. 231, p. 110454.

International Energy Agency (2023), District Heating, available at: https://www.iea.org/energy-system/buildings/district-heating (accessed 27 November 2023).

Krug, R., Mehrmann, V. and Schmidt, M. (2020), Nonlinear optimization of district heating networks, *Optimization and Engineering*, Vol. 19 No. 1, p. 1.

Lund, H., Østergaard, P.A., Nielsen, T.B., Werner, S., Thorsen, J.E., Gudmundsson, O., Arabkoohsar, A. and Mathiesen, B.V. (2021), Perspectives on fourth and fifth generation district heating, *Energy*, Vol. 227, p. 120520.

Mertz, T., Serra, S., Henon, A. and Reneaume, J.-M. (2016), A MINLP optimization of the configuration and the design of a district heating network: Academic study cases, *Energy*, Vol. 117, pp. 450–464.

Morvaj, B., Evins, R. and Carmeliet, J. (2016), Optimising urban energy systems: Simultaneous system sizing, operation and district heating network layout, *Energy*, Vol. 116, pp. 619–636.

Mu, C., Ding, T., Qu, M., Zhou, Q., Li, F. and Shahidehpour, M. (2020), Decentralized optimization operation for the multiple integrated energy systems with energy cascade utilization, *Applied Energy*, Vol. 280, p. 115989.

Newman, R. and Noy, I. (2023), The global costs of extreme weather that are attributable to climate change, *Nature communications*, Vol. 14 No. 1, p. 6103.

Nuytten, T., Claessens, B., Paredis, K., van Bael, J. and Six, D. (2013), Flexibility of a combined heat and power system with thermal energy storage for district heating, *Applied Energy*, Vol. 104, pp. 583–591.

Pfluger, B., Hanßke, A., Ragwitz, M., Sporleder, M., Fritz, M., Kirbach, R., Ruscheinski, F., Steinbach, J., Popovski, E. and Haller, J. (2023), *Wissenschaftliche Transformationsstudie zur Dekarbonisierung der Wärmebereitstellung in der Region Hoyerswerda, Weißwasser und Spremberg bis 2050*.

Rämä, M. and Wahlroos, M. (2018), Introduction of new decentralised renewable heat supply in an existing district heating system, *Energy*, Vol. 154, pp. 68–79.

Sporleder, M., Rath, M. and Ragwitz, M. (2022), Design optimization of district heating systems: A review, *Frontiers in Energy Research*, Vol. 10.

Sporleder, M., Rath, M. and Ragwitz, M. (2024), Solar thermal vs. PV with a heat pump: A comparison of different charging technologies for seasonal storage systems in district heating networks, *Energy Conversion and Management: X*, Vol. 22, p. 100564.

Sporleder, M., Xu, Y., Rath, M., Ragwitz, M. and van Beek, M. (2023), Utilizing Historical Operating Data to Increase Accuracy for Optimal Seasonal Storage Integration and Planning, in Blanco-Marigorta, A.M., Del Rio Gamero, B. and Martel, Noemí Melián, El Kori, Nenna (Eds.), *36th International Conference on Efficiency, Cost, Optimization, Simulation and Environmental Impact of Energy Systems (ECOS 2023), Las Palmas De Gran Canaria, Spain, 25.06.2023 - 30.06.2023*, Curran Associates, Inc., Las Palmas De Gran Canaria, Spain, pp. 2241–2252.

VDI The Association of German Engineers (2012), *Economic efficiency of building installations - Fundamentals and economic calculation* VDI 2067, Beuth Publisher, Berlin, available at: https://www.vdi.de/richtlinien/details/vdi-2067-blatt-1-wirtschaftlichkeit-gebaeudetechnischer-anlagen-grundlagen-und-kostenberechnung-1#:~:text=Die%20Richtlinienreihe%20VDI%202067%20behandelt,Richtlinienreihe%20in%20mehrere%20Bl%C3%A4tter%20gegliedert. (accessed 15 February 2023).

Wirtz, M., Kivilip, L., Remmen, P. and Müller, D. (2020), 5th Generation District Heating: A novel design approach based on mathematical optimization, *Applied Energy*, Vol. 260, p. 114158.

ACKNOWLEDGEMENTS

MS: Conceptualization, Methodology, Validation, Formal Analysis, Data curation, Writing - Original draft preparation, Visualization. MR Supervision, Methodology, Review & Editing. MR Resources, Review & Editing. The project was founded by the ODH@Jülich and the BMBF.

https://doi.org/10.52202/077185-0064